Hindawi Publishing Corporation
Mathematical Problems in Engineering
Volume 2014, Article ID 801628, 11 pages
http://dx.doi.org/10.1155/2014/801628

Research Article

Vehicle Velocity and Roll Angle Estimation with Road and Friction Adaptation for Four-Wheel Independent Drive Electric Vehicle

Linhui Zhao and Zhiyuan Liu

Department of Control Science and Engineering, Harbin Institute of Technology, Harbin 150001, China

Correspondence should be addressed to Linhui Zhao; zhaolinhui@hit.edu.cn

Received 30 April 2014; Accepted 7 October 2014; Published 22 October 2014

Academic Editor: Bo Shen

Vehicle velocity and roll angle are important information for active safety control systems of four-wheel independent drive electric vehicle. In order to obtain robustness estimation of vehicle velocity and roll angle, a novel method is proposed based on vehicle dynamics and the measurement information provided by the sensors equipped in modern cars. The method is robust with respect to different road and friction conditions. Firstly, the dynamic characteristics of four-wheel independent drive electric vehicle are analyzed, and a four-degree-of-freedom nonlinear dynamic model of vehicle and a tire longitudinal dynamic equation are established. The relationship between the longitudinal and lateral friction forces is derived based on Dugoff tire model. The unknown input reconstruction technique of sliding mode observer is used to achieve longitudinal tire friction force estimation. A simple observer is designed for the estimation of the roll angle of the vehicle. And then using the relationship, the estimated longitudinal friction forces and roll angle, a sliding mode observer for vehicle velocity estimation is provided, which does not need to know the tire-road friction coefficient and road angles. Finally, the proposed method is evaluated experimentally under a variety of maneuvers and road conditions.

1. Introduction

Vehicle active safety control systems such as yaw stability control system and roll stability control system can significantly reduce the number of road accidents [1–3]. However, these systems usually depend upon information about vehicle velocity, yaw rate, and roll angle. Generally, the yaw rate is measurable, but the vehicle velocity and roll angle cannot be measured directly in modern cars due to the cost and reliability issues. As a consequence, they must be estimated, and the accurate and reliable vehicle velocity and roll angle information is very important for the vehicle active safety control systems [4, 5]. Since the wheel torques of four-wheel independent drive electric vehicle can be obtained easily, the higher accuracy of vehicle velocity estimation compared to conventional vehicles can be achieved, which should be used to improve the performance of vehicle active safety control systems.

In [6], an extended Kalman filter is used to estimate vehicle velocity and friction forces. Since a random walk is chosen to model each friction force, the estimation accuracy may be degraded when the friction forces are time-varying during braking and driving. In addition, as the vehicle model is significantly nonlinear, model errors related to currently estimated state may be introduced by linearization. A nonlinear observer for vehicle velocity estimation with stability guarantees, based on acceleration and yaw rate measurements in addition to wheel angular velocity and steering wheel angle measurements, is investigated in [7]. But the wheel angular velocity measurements are transformed to measurements of longitudinal velocity and used in the feedback term of the observer. This is based on an assumption of zero tire longitudinal and lateral slips. So the measurements will contain large errors and deteriorate the estimate of longitudinal velocity when the tire slips are high. Unfortunately, the tire slips usually are high during braking and steering especially on low friction surfaces. Moreover, the longitudinal velocity observer gains must be determined at each sample time. This has an adverse effect on the real-time performance of the observer. In [8], a sliding mode observer is suggested to

estimate vehicle sideslip angle, while a linear lateral friction model is used and longitudinal friction forces are treated as inputs of the observer. However, the linear relationship representing lateral friction force is not sufficiently accurate anymore for lateral acceleration above 4 m/s^2 and large tire sideslip angle, and longitudinal friction force is not always available in modern cars [9]. However, the researches above assume that the road grade angle and bank angle are zero or are known for accurate estimation of vehicle velocity. The road angles are nonzero if the road is nonflat and then have significant effect in both vehicle dynamics and acceleration measurements [10]. A method for identifying road bank angle and vehicle roll angle separately using measurements from global positioning system and inertial navigation system sensors is developed in [11]. In [12], the lateral tire force sensors are used to estimate the vehicle sideslip angle and roll angle for four-wheel independent drive electric vehicle, and high estimation accuracy is achieved. But the sensors mentioned above are expensive for modern cars. In [13], the estimation of the road grade and bank angles is discussed based on vehicle longitudinal and lateral dynamics and the assumption that the angles vary slowly enough compared to the dynamics of the system; the effect of the roll angle has not been considered in this paper.

In this paper, using the measurements from the existing sensors equipped in the four-wheel independent drive electric vehicle, including the wheel angular velocities, longitudinal and lateral accelerations, yaw rate, roll rate, wheel steering angles, and wheel torques, a method for vehicle velocity and roll angle estimation with road and friction adaptation is proposed based on the nonlinear vehicle dynamics and Dugoff tire model. The proposed method is evaluated experimentally under a variety of maneuvers and road conditions.

2. Vehicle Model

As shown in Figures 1 and 2, a vehicle maneuvering and roll model is used to design the vehicle velocity and roll angle observers. This model has four degrees of freedom for longitudinal motion, lateral motion, yaw motion, and roll motion of the vehicle. During handling maneuvers on smooth roads, the vehicle roll motion is primarily induced by lateral acceleration [14]. Based on this assumption, a body-fixed coordinate system with the origin at the vehicle center of gravity (COG) is used to set up the model, and the kinematic relationships among the vehicle velocity, yaw rate, roll angle, and acceleration are as follows:

$$\begin{aligned} \dot{v}_x &= r v_y + a_x - g \sin\theta_r, \\ \dot{v}_y &= a_y - r v_x + g \sin(\phi_v + \phi_r), \\ J_x \ddot{\phi}_v + C_{\text{roll}} \dot{\phi}_v + K_{\text{roll}} \phi_v &= m_s a_y h_{\text{roll}}, \\ \dot{r} &= \frac{M_z}{J_z}, \end{aligned} \tag{1}$$

where v_x and v_y are the longitudinal and lateral velocities of vehicle COG. r is the yaw rate. θ_r and ϕ_r denote the road grade and bank angles. The effect between the road grade and bank angle is not considered in this paper. g is the gravitational constant. ϕ_v is the roll angle as a result of vehicle lateral motion by steering maneuvers. a_x and a_y are the longitudinal and lateral accelerations measurements from the sensors attached to the vehicle body and aligned with the body-fixed coordinate system, and they will be different from the actual accelerations of the COG when there are nonzero road grade angle and bank angle. J_x is the vehicle moment of inertia about longitudinal axis. C_{roll} is the roll stiffness and K_{roll} is the roll damping. m_s is the sprung mass of the vehicle and h_{roll} is the height of the roll center. J_z is the vehicle moment of inertia about vertical axis. M_z is the torque about vertical axis.

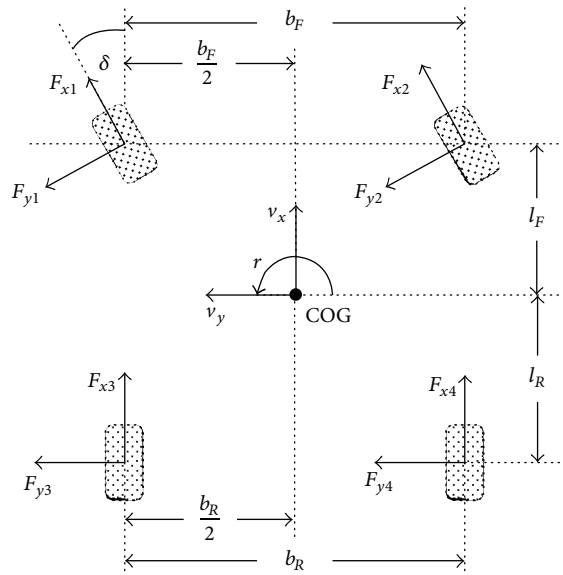

Figure 1: Vehicle maneuvering model.

Due to the presence of measurement errors such as biases and noise from the sensors, some feedback should be used to make the estimated results converge, and then the vehicle dynamics is introduced into the vehicle model (1). According to Figure 1, the force balances in the direction of the longitudinal and lateral axis as well as the torque balance about the vertical axis are given by

$$\begin{aligned} a_x &= \frac{F_x}{m}, \qquad a_y = \frac{F_y}{m}, \\ M_z &= l_F \left((F_{x1} + F_{x2}) \sin\delta + (F_{y1} + F_{y2}) \cos\delta \right) \\ &\quad - l_R (F_{y3} + F_{y4}) \\ &\quad + \frac{b_F \left((F_{y1} - F_{y2}) \sin\delta - (F_{x1} - F_{x2}) \cos\delta \right)}{2} \\ &\quad - \frac{b_R (F_{x3} - F_{x4})}{2}, \end{aligned} \tag{2}$$

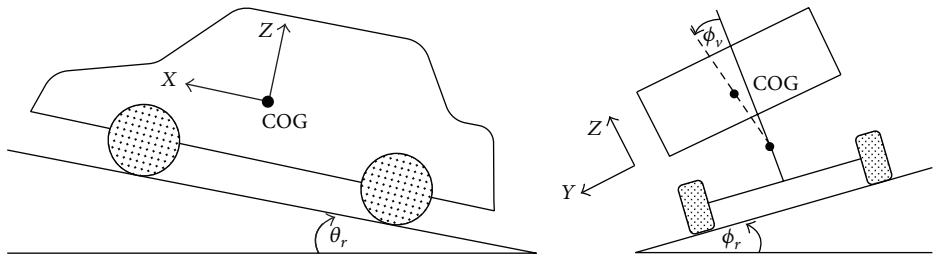

(a) Force induced by road grade angle (b) Vehicle roll model

Figure 2: Force induced by road grade angle and vehicle roll model.

with

$$\begin{aligned} F_x &= (F_{x1} + F_{x2}) \cos\delta \\ &\quad - (F_{y1} + F_{y2}) \sin\delta + F_{x3} + F_{x4} - C_x v_x^2, \\ F_y &= (F_{x1} + F_{x2}) \sin\delta \\ &\quad + (F_{y1} + F_{y2}) \cos\delta + F_{y3} + F_{y4}, \end{aligned} \tag{3}$$

where the effect of wheel rolling resistance forces is ignored. m denotes the total mass of the vehicle. δ is the front wheel steering angle and can be obtained from the measured steering wheel angle directly. C_x represents the aerodynamic resistances coefficient. l_F and l_R are the distances from the vehicle COG to the front and rear axle and b_F and b_R are the front and rear track width. F_{xi} and F_{yi} are the longitudinal and lateral friction forces of the ith wheel, and i is 1, 2, 3, and 4 and represents four wheels, respectively.

The nonlinearity of vehicle tires will become a critical factor during emergency maneuvers in which the linear tire model is not sufficiently accurate anymore. To account for the nonlinearities of the tire friction force, Dugoff tire model [15] is used in this paper, and the longitudinal friction force F_{xi} and the lateral friction force F_{yi} of the ith wheel in (3) are given as

$$\begin{aligned} F_{xi} &= \frac{C_\sigma \sigma_i}{1 + \sigma_i} f(\lambda_i), \\ F_{yi} &= \frac{C_\alpha \tan\alpha_i}{1 + \sigma_i} f(\lambda_i), \end{aligned} \tag{4}$$

where C_σ and C_α are the longitudinal and cornering stiffness of the tire. σ_i and α_i denote the tire longitudinal slip and the tire sideslip angle of the ith wheel. The definition and calculation method of these variables are shown in [16]. The variable λ_i and the function $f(\lambda_i)$ are defined as

$$\begin{aligned} \lambda_i &= \frac{\mu F_{zi} (1 + \sigma_i)}{2\sqrt{(C_\sigma \sigma_i)^2 + (C_\alpha \tan\alpha_i)^2}}, \\ f(\lambda_i) &= \begin{cases} 1 & \lambda_i \geq 1, \\ (2 - \lambda_i)\lambda_i & \lambda_i < 1, \end{cases} \end{aligned} \tag{5}$$

where μ is the tire-road friction coefficient. F_{zi} is the normal force for each wheel and is calculated as

$$\begin{aligned} F_{z1} &= \frac{mgl_R - ma_x h}{2(l_F + l_R)} - \frac{ma_y l_R h}{(l_F + l_R) b_F}, \\ F_{z2} &= \frac{mgl_R - ma_x h}{2(l_F + l_R)} + \frac{ma_y l_R h}{(l_F + l_R) b_F}, \\ F_{z3} &= \frac{mgl_F + ma_x h}{2(l_F + l_R)} - \frac{ma_y l_F h}{(l_F + l_R) b_R}, \\ F_{z4} &= \frac{mgl_F + ma_x h}{2(l_F + l_R)} + \frac{ma_y l_F h}{(l_F + l_R) b_R}, \end{aligned} \tag{6}$$

where h denotes the height of vehicle COG.

For four-wheel independent drive electric vehicle, the torque balance of the wheel i is

$$J_R \dot{\omega}_i = -R_{\text{eff}} F_{xi} + T_i, \tag{7}$$

where J_R is the moment of inertia of the wheel. R_{eff} is the effective radius of the wheel. ω_i and T_i denote the angular velocity and the wheel torque of the ith wheel.

3. Observer Design

3.1. Estimation of Friction Force. In the wheel longitudinal dynamic equation (7), the wheel angular velocity ω_i is measurable, and the wheel torque T_i can be obtained directly from the motor control system of four-wheel independent drive electric vehicle. So (7) can be described in state space form as follows:

$$\dot{x} = Bu + Pd, \qquad y = x, \tag{8}$$

where $x = \omega_i$ is the system state and $u = T_i$ is the control input. $d = F_{xi}$ is unknown and bounded input. y is the measurement output. $B = 1/J_R$, and $P = -R_{\text{eff}}/J_R$.

Obviously, the unknown input d is observable with respect to the measurement output y in the system (8). So the estimation problem of longitudinal friction force can be described as to reconstruct the unknown input d of the system (8) from the measurement output y.

The sliding mode observer, through sliding surface design and equivalent control concept, has been proven to be an

effective approach for handling the systems with disturbances and modeling uncertainties. Based on the unknown input estimation technique of the sliding mode observer, this paper proposed the following observer for longitudinal friction force estimation:

$$\begin{aligned} \dot{\widehat{x}} &= Bu + l\left(y - \widehat{x}\right) + Pv, \\ v &= -P^{-1}\rho \operatorname{sign}\left(\widehat{x} - x\right), \end{aligned} \tag{9}$$

where ρ is the sliding mode gain. l denotes the feedback gain, and the Luenberger type of feedback loop in the observer is used to ensure the stability of the observer.

If we define the estimation error $\tilde{x} = x - \widehat{x}$ and the Lyapunov function $V = \tilde{x}^2/2$, the stability results for error dynamics of the observer (9) then can be obtained directly. If the gains ρ and l are chosen such that

$$\rho > \left\| -l\tilde{x} + Pd \right\|, \tag{10}$$

it will have $\dot{V} < 0$. Hence the dynamics $\tilde{x}$ reaches the sliding mode in finite time and stays thereafter.

Once the state of the observer (9) converges to the actual state, the longitudinal friction force can be reconstructed according to (9) as follows:

$$\begin{aligned} \widehat{F}_{xi} = \widehat{d} &\approx \left(-P^{-1}\rho \operatorname{sign}\left(\widehat{x} - x\right)\right)_{\text{eq}} \\ &= \frac{J_R}{R_{\text{eff}}}\rho \frac{\widehat{\omega}_i - \omega_i}{\left|\widehat{\omega}_i - \omega_i\right| + \eta}, \end{aligned} \tag{11}$$

where η is a small positive real number and affects the accuracy of the unknown input estimation.

Actually, the longitudinal and lateral friction forces can be calculated directly using the Dugoff tire model. But the calculation of the longitudinal and lateral friction forces needs to know the tire-road friction coefficient, which usually cannot be measured based on the sensors equipped in modern cars. The tire-road friction coefficient not only depends on the road conditions (such as asphalt, ice and snow, etc.), but also is affected by tire materials, ambient temperature, and other factors. The relationship between them is very difficult to be described by mathematical model. So the estimation of the tire-road friction coefficient is not an easy task [17].

According to the Dugoff tire model (4) and (5), the relationship between the longitudinal and lateral friction forces can be derived as follows:

$$F_{yi} = \frac{C_\alpha \tan \alpha_i}{C_\sigma \sigma_{xi}} F_{xi}. \tag{12}$$

Based on this relationship, the lateral friction force can be calculated using the estimated longitudinal friction force and vehicle states directly, which did not need the tire-road friction coefficient.

3.2. Estimation of Roll Angle. According to the vehicle roll model shown in Figure 2(b) and (1), the model used in this paper for roll angle estimation is given by

$$\begin{aligned} \dot{\phi}_v &= \varphi, \\ \dot{\varphi} &= -\frac{C_{\text{roll}}\varphi}{J_x} - \frac{K_{\text{roll}}\phi_v}{J_x} + \frac{m_s h_{\text{roll}} a_y}{J_x}, \end{aligned} \tag{13}$$

where φ denotes the roll rate of the vehicle.

Since the lateral acceleration and roll rate usually are measurable in modern cars, the observer for roll angle estimation in this paper is proposed as follows:

$$\begin{aligned} \dot{\widehat{\phi}}_v &= \varphi + k_\phi\left(\varphi - \widehat{\varphi}\right), \\ \dot{\widehat{\phi}} &= -\frac{C_{\text{roll}}\varphi}{J_x} - \frac{K_{\text{roll}}\widehat{\phi}_v}{J_x} + \frac{m_s h_{\text{roll}} a_y}{J_x} + k_\varphi\left(\varphi - \widehat{\phi}\right), \end{aligned} \tag{14}$$

where k_ϕ and k_φ are the feedback gain and can be determined by the pole placement method.

3.3. Estimation of Vehicle Velocity. According to the vehicle kinematic model (1) and dynamic model (2), the model used in this paper for vehicle velocity estimation is given by

$$\begin{aligned} \dot{v}_x &= rv_y + a_x - g\sin\theta_r, \\ \dot{v}_y &= a_y - rv_x + g\sin\phi_v + g\sin\phi_r, \\ \dot{r} &= \frac{M_z}{J_z}. \end{aligned} \tag{15}$$

Since the roll angle of the vehicle and the road bank angle usually are small, the assumption $\sin(\phi_v + \phi_r) = \sin\phi_v + \sin\phi_r$ is made in the above equation. The obtaining of the road grade angle and bank angle is not an easy task based on the sensors equipped in modern cars. The terms $g\sin\theta_r$ and $g\sin\phi_r$ are considered as unknown and bounded inputs of the system in this paper.

In modern cars, the longitudinal acceleration, lateral acceleration, and yaw rate usually are measurable. Taking into account the model mismatch of the nonlinear vehicle dynamics and the presence of measurement errors such as biases and noise from the existing sensors equipped in vehicle, the difference between the calculation value of longitudinal and lateral accelerations based on nonlinear vehicle dynamic model and the measurement value provided by the sensor as a feedback term is introduced to improve the estimation accuracy of the vehicle velocity. And the estimation

method of vehicle velocity based on the sliding mode observer is proposed in this paper as follows:

$$\begin{aligned}
\dot{\widehat{v}}_x &= r\widehat{v}_y + a_x - l_x\left(a_x - \frac{\widehat{F}_x}{m}\right) - \rho_x \operatorname{sign}\left(a_x - \frac{\widehat{F}_x}{m}\right),\\
\dot{\widehat{v}}_y &= -r\widehat{v}_x + a_y + g\sin\phi_v - l_y\left(a_y - \frac{\widehat{F}_y}{m}\right)\\
&\quad - \rho_y \operatorname{sign}\left(a_y - \frac{\widehat{F}_y}{m}\right),\\
\dot{\widehat{r}} &= \frac{\widehat{M}_z}{J_z} + l_r\left(r - \widehat{r}\right) + \rho_r \operatorname{sign}\left(r - \widehat{r}\right),
\end{aligned} \tag{16}$$

where l_i and ρ_i, $i = x, y, r$, are the feedback gain and siding mode gain of the observer. $\widehat{F}_x$, $\widehat{F}_y$, and $\widehat{M}_z$ are estimated values of F_x, F_y, and M_z, which can be calculated based on (3) using the estimated longitudinal friction forces and vehicle states. The estimated roll angle of the vehicle from the observer (14) is considered as an input of the observer (16). The observer defined by (16) copies the structure of the Luenberger observer, with disturbances replaced by their corresponding sliding mode terms. The main aim is to show that state estimation will be totally insensitive to disturbances, if and only if there exists a sliding mode term to track every unknown input.

The structure of the roll angle and vehicle velocity observers proposed in this paper for four-wheel independent drive electric vehicle is illustrated in Figure 3. Based on (11), the longitudinal friction force of the four wheels can be obtained using the measured wheel angular velocity and wheel torque, and then the lateral friction forces are achieved according to (12), which does not need to know the tire-road friction coefficient. In other words, the calculation of the friction forces in the vehicle velocity observer can adapt with road friction condition. At the same time, the road grade angle and bank angle can be constructed together with the estimation of the vehicle velocity.

To avoid excessive chattering, the sign(·) in the observer (16) is replaced by $\operatorname{sign}_{\mathrm{eq}}(\cdot)$, which is defined as follows:

$$\operatorname{sign}_{\mathrm{eq}}(e, \eta) = \frac{e}{|e| + \eta}, \tag{17}$$

where e is the estimation error and η is a small positive scalar to adjust the slope of the function $\operatorname{sign}_{\mathrm{eq}}(\cdot)$.

In the following, the selection of the feedback gains and sliding mode gains to guarantee the stability of the observer (16) should be discussed. Define

$$\begin{aligned}
k_x &= l_x + \frac{\rho_x}{\left|a_x - \widehat{F}_x/m\right| + \eta},\\
k_y &= l_y + \frac{\rho_y}{\left|a_y - \widehat{F}_y/m\right| + \eta},\\
k_r &= l_r + \frac{\rho_r}{\left|r - \widehat{r}\right| + \eta}.
\end{aligned} \tag{18}$$

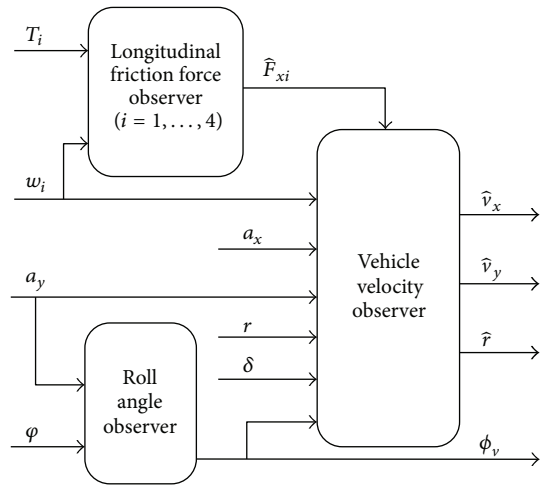

Figure 3: The structure of the proposed roll angle and vehicle velocity observers.

Substituting (17) and (18) into (16), the vehicle velocity observer equations can be rewritten as

$$\begin{aligned}
\dot{\widehat{v}}_x &= r\widehat{v}_y + a_x - k_x\left(a_x - \frac{\widehat{F}_x}{m}\right),\\
\dot{\widehat{v}}_y &= -r\widehat{v}_x + a_y + g\phi - k_y\left(a_y - \frac{\widehat{F}_y}{m}\right),\\
\dot{\widehat{r}} &= \frac{\widehat{M}_z}{J_z} + k_r\left(r - \widehat{r}\right).
\end{aligned} \tag{19}$$

Define the estimation errors $\widetilde{v}_x = v_x - \widehat{v}_x$, $\widetilde{v}_y = v_y - \widehat{v}_y$, and $\widetilde{r} = r - \widehat{r}$; the error dynamics of the observer (19) is given by

$$\begin{aligned}
\dot{\widetilde{v}}_x &= r\widetilde{v}_y + k_x\left(a_x - \frac{\widehat{F}_x}{m}\right) + u_1,\\
\dot{\widetilde{v}}_y &= -r\widetilde{v}_x + k_y\left(a_y - \frac{\widehat{F}_y}{m}\right) + u_2,\\
\dot{\widetilde{r}} &= \frac{\left(M_z - \widehat{M}_z\right)}{J_Z} - k_r\widetilde{r},
\end{aligned} \tag{20}$$

with $u_1 = -g\sin\theta_r$, $u_2 = g\sin\phi_r$. The values of u_1 and u_2 are bounded because the road grade angle θ_r and the road bank angle ϕ_r usually are small according to the real road condition.

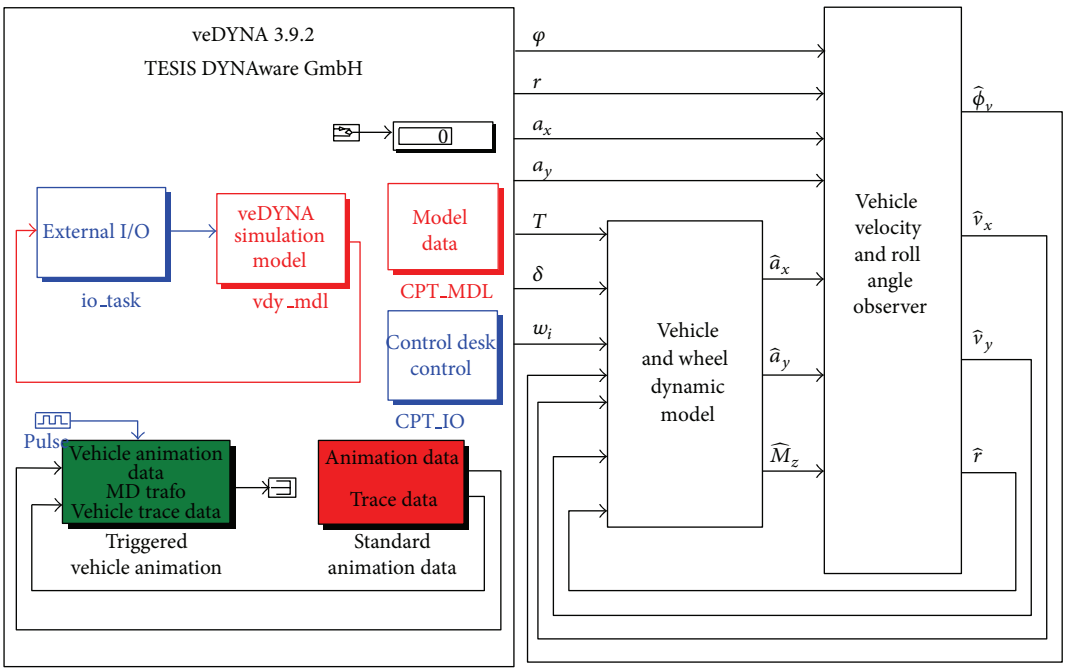

Figure 4: The structure of the simulation system.

Define the Lyapunov function

$$V = \frac{1}{2}\tilde{v}_x^2 + \frac{1}{2}\tilde{v}_y^2 + \frac{1}{2}\tilde{r}^2; \tag{21}$$

its time derivative along the trajectories of (18) is given by

$$\begin{aligned}\dot{V} &= k_x\tilde{v}_x\left(a_x - \frac{\widehat{F}_x}{m}\right) + u_1\tilde{v}_x + k_y\tilde{v}_y\left(a_y - \frac{\widehat{F}_y}{m}\right)\\ &\quad + u_2\tilde{v}_x + \frac{\tilde{r}\left(M_z - \widehat{M}_z\right)}{J_Z} - k_r\tilde{r}^2.\end{aligned} \tag{22}$$

According to the analysis method in the authors' previous published literature [16], the following results can be obtained directly:

$$\dot{V} \le -|\tilde{\mathbf{x}}|^T A\,|\tilde{\mathbf{x}}| + \|\tilde{\mathbf{x}}\|\,\|\mathbf{u}\|, \tag{23}$$

where $|\tilde{\mathbf{x}}| = (|\tilde{v}_x|, |\tilde{v}_y|, |\tilde{r}|)^T$, $\mathbf{u} = (u_1, u_2)^T$, and the matrix A is defined as

$$A = \begin{bmatrix} k_x c_1 & -\dfrac{k_x c_2 + k_y c_4}{2} & -\dfrac{k_x c_3 + c_7}{2} \\ -\dfrac{k_x c_2 + k_y c_4}{2} & k_y c_5 & -\dfrac{k_y c_6 + c_8}{2} \\ -\dfrac{k_x c_3 + c_7}{2} & -\dfrac{k_y c_6 + c_8}{2} & k_r - c_9 \end{bmatrix}, \tag{24}$$

and c_i, $i = 1, 2, \ldots, 9$, is positive constants. So if the observer gains k_j, $j = x, y, r$, are chosen as

$$\begin{gathered} k_1 > 0, \\ \frac{2c_1c_5 - c_2c_4 - c_{10}}{c_4^2}k_1 < k_2 < \frac{2c_1c_5 - c_2c_4 + c_{10}}{c_4^2}k_1, \\ k_3 > c_9 + \frac{c_{11}}{4k_1k_2c_1c_5 - (k_1c_2 + k_2c_4)^2}, \end{gathered} \tag{25}$$

with

$$\begin{aligned} c_{10} &= \sqrt{4c_1c_5(c_1c_5 - c_2c_4)}, \\ c_{11} &= k_1c_1(k_2c_6 + c_8)^2 + k_2c_5(k_1c_3 + c_7)^2 \\ &\quad + (k_1c_2 + k_2c_4)(k_1c_3 + c_7)(k_2c_6 + c_8), \end{aligned} \tag{26}$$

the matrix A is positive definite, and then

$$\begin{aligned} \dot{V} &\le -\lambda_{\min}(A)\,\|\tilde{\mathbf{x}}\|^2 + \|\tilde{\mathbf{x}}\|\,\|\mathbf{u}\| \\ &\le -\lambda_{\min}(A)(1-\theta)\,\|\tilde{\mathbf{x}}\|^2, \\ &\qquad \forall\,\|\tilde{\mathbf{x}}\| \ge \frac{\|\mathbf{u}\|}{\lambda_{\min}(A)\,\theta}, \end{aligned} \tag{27}$$

where $0 < \theta < 1$ and $\lambda_{\min}(A)$ denotes the minimum eigenvalue of the matrix A.

From the above discussion, it is clear that if the road is flat, the road grade angle and bank angle are zero, and $\mathbf{u} = 0$; the inequality (23) can be rewritten as $\dot{V} \le -|\tilde{\mathbf{x}}|^T A|\tilde{\mathbf{x}}|$; then the observer error dynamics (20) is asymptotically stable. For $\mathbf{u} \ne 0$, the inequality (23) clearly implies that the observer error dynamics (20) is input-to-state stability (ISS) with respect to $\mathbf{u}$.

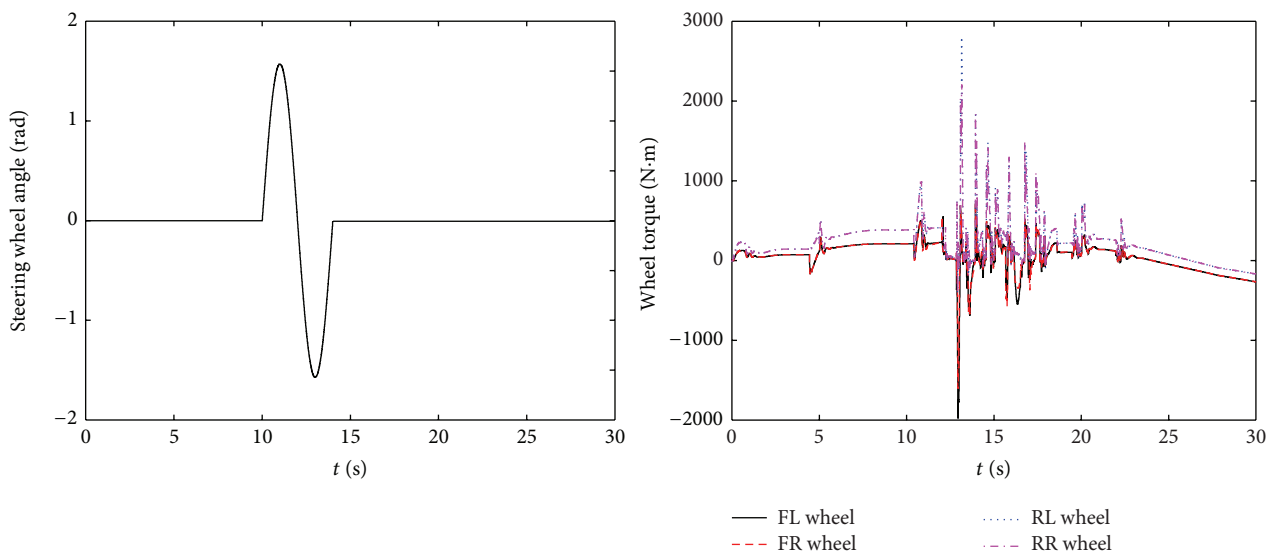

Figure 5: The steering wheel angle and wheel torque in the sudden steering maneuver.

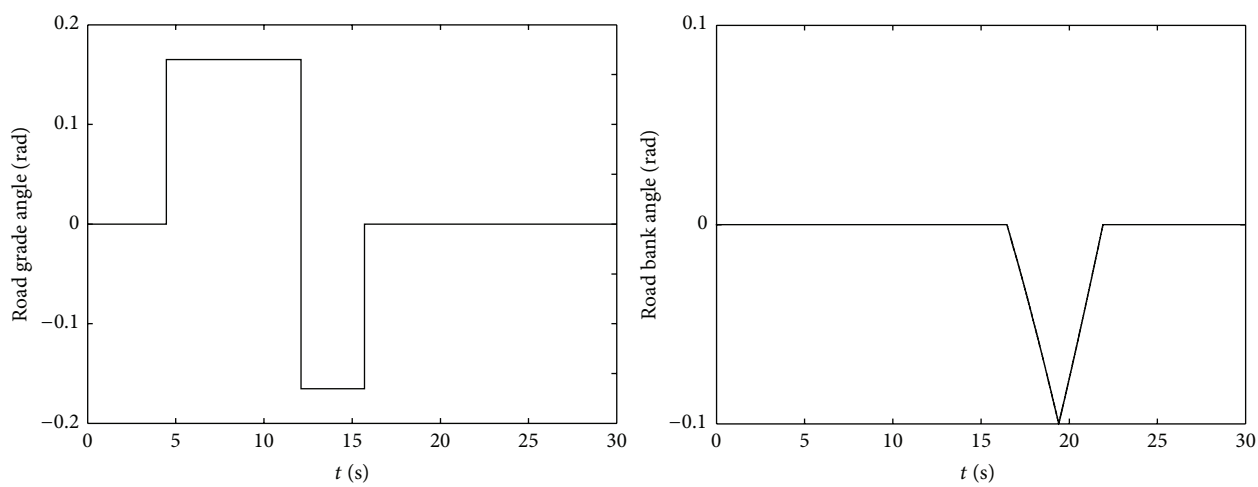

Figure 6: The road grade angle and bank angle in the sudden steering maneuver.

4. Simulation Results

As shown in Figure 4, by modifying some related part based on the existing model in veDYNA, a high-precision vehicle dynamics simulation system for four-wheel independent drive electric vehicle has been built in this paper. The veDYNA simulator, developed by the group of companies TESIS, is the software which provides an integrated development environment for quickly conducting vehicle simulation and control algorithm design, especially for chassis/driveline modeling and simulation. The vehicle parameters used in the veDYNA and observers proposed in this paper are the same as in [11].

To represent the most likely cause of error in true data acquisition, zero-mean-value random measure noises with Gaussian distribution are introduced into the vehicle acceleration, yaw rate, and roll rate measurements during the course of simulation. The performance of the observers is evaluated under a sudden steering maneuver on a high friction surface ($\mu = 0.9$) and a slalom maneuver on a low friction surface ($\mu = 0.45$), and the test vehicle drives on nonflat roads in each maneuver, respectively.

In the sudden steering maneuver, the longitudinal vehicle velocity strongly varies. As shown in Figure 5, the duration of vehicle acceleration and brake has been included, and the steering wheel angle changes from zero to 90 degrees during 1 second when vehicle is running at high speed. The road grade angle and bank angle are shown in Figure 6. In Figures 7 and 8, the estimated roll angle, yaw rate, and vehicle velocities from the proposed observers are compared to those of the veDYNA simulator, respectively.

The second test is a slalom maneuver on a low friction surface. The steering wheel angle and wheel torque measurements are shown in Figure 9. In this test, the steering

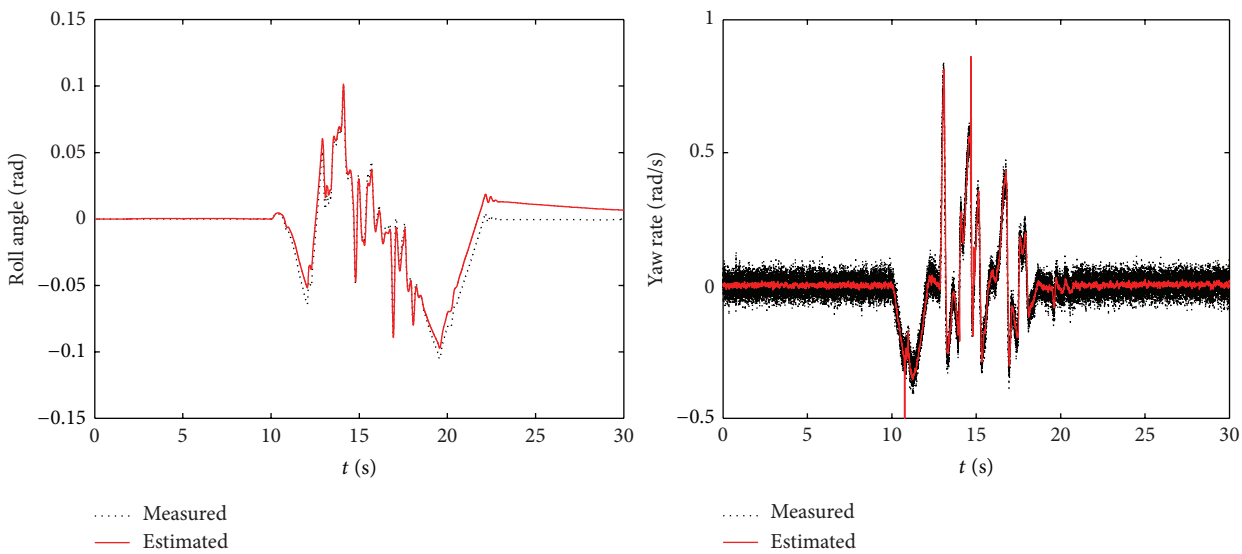

Figure 7: The measured and estimated vehicle roll angle and yaw rate in the sudden steering maneuver.

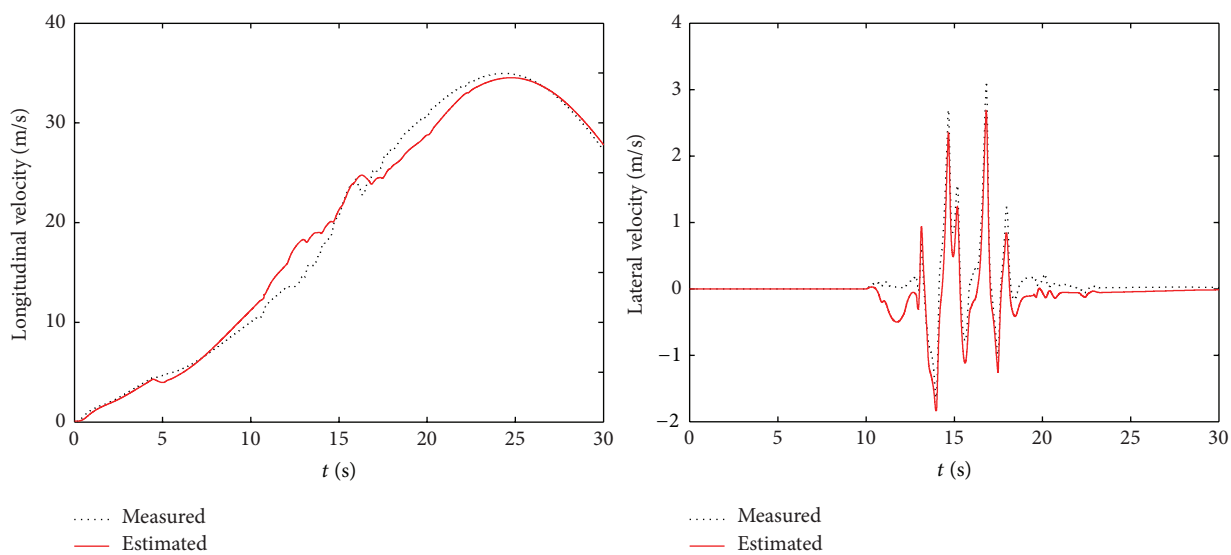

Figure 8: The measured and estimated vehicle velocities in the sudden steering maneuver.

wheel angle turns quickly during the vehicle running, and the amplitude of the steering wheel angle is 30 degrees. The road grade angle and bank angle in this test are shown in Figure 10. Figures 11 and 12 show the roll angle, yaw rate, and vehicle velocities estimation results from the proposed observer and the veDYNA simulator.

As shown in Figures 8 and 12, the estimated vehicle velocities from the proposed observer with respect to different road angles and surface conditions are very close to the values of the veDYNA simulator, and the vehicle velocity observer does not need to know the road angles and the tire-road friction coefficient. This is to be expected since the estimated longitudinal friction forces and the relationship between the longitudinal and lateral friction forces are used in the vehicle velocity observer proposed in this paper. At the same time, the sliding mode terms are used in the vehicle velocity observer as a "tracking element" for the unknown inputs caused by road grade angle and bank angle, which are difficult to be measured. From Figures 7 and 11, it can be seen that the estimation of the roll angle has also achieved good performance. It also can be seen that the estimation of yaw rate contains relatively more noise. This is mainly induced by the noise of measurement, which can be decreased by a low-pass filter, such as one with a transfer function of $1/(s + a)$, where a is a constant.

5. Conclusion

In this paper, a roll angle observer and a vehicle velocity observer have been proposed for four-wheel independent

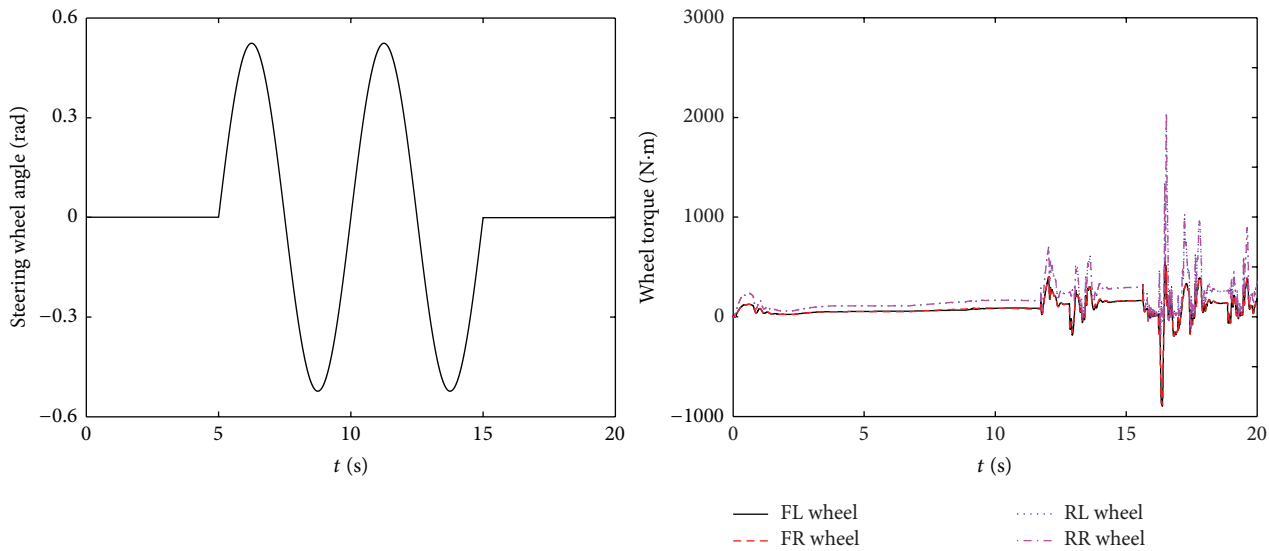

Figure 9: The steering wheel angle and wheel torque in the slalom maneuver.

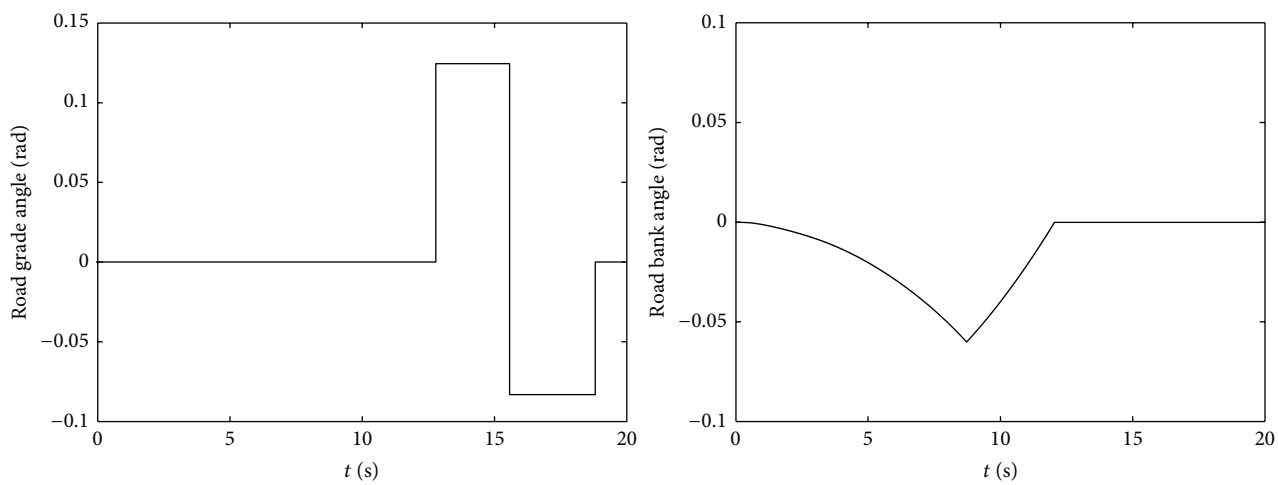

Figure 10: The road grade angle and bank angle in the slalom maneuver.

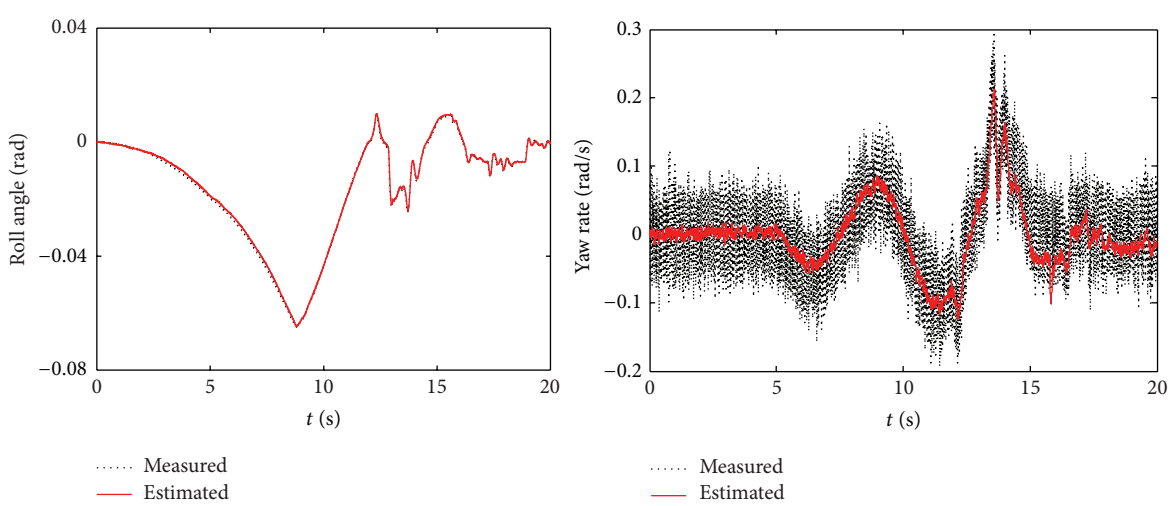

Figure 11: The measured and estimated vehicle roll angle and yaw rate in the slalom maneuver.

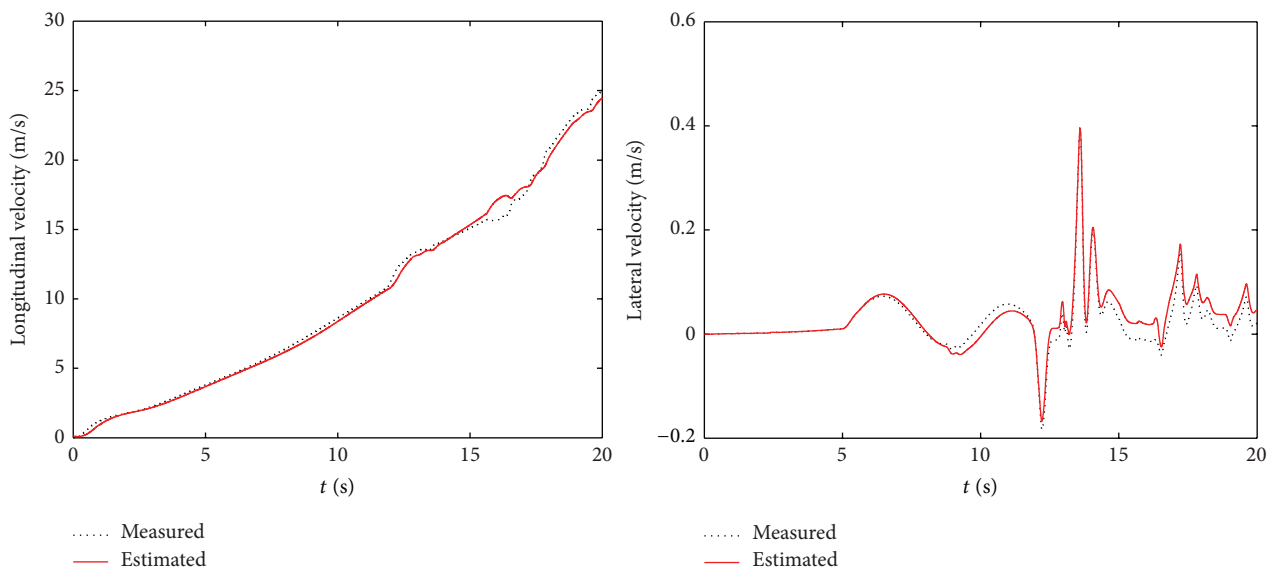

Figure 12: The measured and estimated vehicle velocities in the slalom maneuver.

drive electric vehicle without needing to measure or estimate the road angles and surface conditions, using the available measurements in modern cars including the wheel angular velocities, longitudinal and lateral accelerations, yaw rate, roll rate, wheel steering angles, and wheel torques. The proposed observers have been validated on a high-precision vehicle dynamics simulation system based on veDYNA, and the simulation results show that good performance of the proposed observers has been achieved. Using the estimated vehicle velocities, the vehicle body sideslip angle can be calculated directly, which is also useful for the automotive chassis control systems.

Conflict of Interests

The authors declare that there is no conflict of interests regarding the publication of this paper.

Acknowledgments

This work was supported by the National Natural Science Foundation of China (no. 61104060) and the China Postdoctoral Science Foundation (no. 2014M551244).

References

[1] H. F. Grip, L. Imsland, T. A. Johansen, T. I. Fossen, J. C. Kalkkuhl, and A. Suissa, "Nonlinear vehicle side-slip estimation with friction adaptation," *Automatica*, vol. 44, no. 3, pp. 611–622, 2008.

[2] S.-E. Zhao, Y. Li, and X. Qu, "Vehicle chassis integrated control based on multimodel and multilevel hierarchical control," *Mathematical Problems in Engineering*, vol. 2014, Article ID 248676, 13 pages, 2014.

[3] S. Melzi and E. Sabbioni, "On the vehicle sideslip angle estimation through neural networks: numerical and experimental results," *Mechanical Systems and Signal Processing*, vol. 25, no. 6, pp. 2005–2019, 2011.

[4] K. T. Leung, J. F. Whidborne, D. Purdy, and P. Barber, "Road vehicle state estimation using low-cost GPS/INS," *Mechanical Systems and Signal Processing*, vol. 25, no. 6, pp. 1988–2004, 2011.

[5] R. Wang, G. Yin, and J. Wang, "Vehicle lateral velocity and tire-road friction coefficient estimation," in *Proceedings of the 5th ASME Annual Dynamic Systems and Control Conference*, pp. 495–502, Fort Lauderdale, Fla, USA, October 2012.

[6] M. A. Wilkin, D. C. Crolla, M. C. Levesley et al., "Design of a robust tyre force estimator using an extended Kalman filter," in *Society of Automotive Engineers (SAE) World Congress*, Detroit, Mich, USA, 2005, Paper no. 2005-01-0402.

[7] L. Imsland, T. A. Johansen, T. I. Fossen, H. F. Grip, J. C. Kalkkuhl, and A. Suissa, "Vehicle velocity estimation using nonlinear observers," *Automatica*, vol. 42, no. 12, pp. 2091–2103, 2006.

[8] J. Stéphant, A. Charara, and D. Meizel, "Evaluation of a sliding mode observer for vehicle sideslip angle," *Control Engineering Practice*, vol. 15, no. 7, pp. 803–812, 2007.

[9] H. Shraim, B. Ananou, L. Fridman, H. Noura, and M. Ouladsine, "Sliding mode observers for the estimation of vehicle parameters, forces and states of the center of gravity," in *Proceedings of the 45th IEEE Conference on Decision and Control (CDC '06)*, pp. 1635–1640, San Diego, Calif, USA, December 2006.

[10] Y. Sebsadji, S. Glaser, S. Mammar, and J. Dakhlallah, "Road slope and vehicle dynamics estimation," in *Proceedings of the American Control Conference (ACC '08)*, pp. 4603–4608, Washington, D.C., USA, June 2008.

[11] J. Ryu and J. C. Gerdes, "Estimation of vehicle roll and road bank angle," in *Proceedings of the American Control Conference*, vol. 3, pp. 2110–2115, IEEE, Boston, Mass, USA, July 2004.

[12] K. Nam, S. Oh, H. Fujimoto, and Y. Hori, "Estimation of sideslip and roll angles of electric vehicles using lateral tire force sensors through RLS and kalman filter approaches," *IEEE Transactions on Industrial Electronics*, vol. 60, no. 3, pp. 988–1000, 2013.

[13] H. F. Grip, L. Imsland, T. A. Johansen, J. C. Kalkkuhl, and A. Suissa, "Estimation of road inclination and bank angle in automotive vehicles," in *Proceedings of the American Control Conference (ACC '09)*, pp. 426–432, St. Louis, Mo, USA, June 2009.

[14] A. Hac, T. Brown, and J. Martens, "Detection of vehicle rollover," Paper 2004-01-1757, Society of Automotive Engineers (SAE) World Congress, Michigan, Mich, USA, 2004.

[15] H. Dugoff, P. S. Fancher, and L. Segel, "An analysis of tire traction properties and their influence on vehicle dynamic performance," *SAE Transactions*, vol. 79, pp. 341–366, 1970.

[16] L. H. Zhao, Z. Y. Liu, and H. Chen, "Design of a nonlinear observer for vehicle velocity estimation and experiments," *IEEE Transactions on Control Systems Technology*, vol. 19, no. 3, pp. 664–672, 2011.

[17] R. Wang and J. Wang, "Tire-road friction coefficient and tire cornering stiffness estimation based on longitudinal tire force difference generation," *Control Engineering Practice*, vol. 21, no. 1, pp. 65–75, 2013.